Decisions in Economics and Finance
https://doi.org/10.1007/s10203-024-00491-9

A dynamically consistent discretization method for the Goodwin model with nonlinear Phillips curve. Comparing qualitative and quantitative dynamics

M. M. Baldi[1] · **M. Guzowska**[2] · **E. Michetti**[1]

Received: 30 January 2024 / Accepted: 13 October 2024

Abstract
The Goodwin model is a widely used economic growth model able to explain endogenous fluctuations in employment rate and wage share; in its initial version, the standard Phillips curve is used. In the present work, we suggest a revised Phillips curve that takes into account how the wage share influences the rate of changes of the wage itself thus obtaining a continuous-time modified Goodwin model. Since applying models to real data often requires working in a discrete-time setup, we then move from the continuous-time to the discrete-time version of the proposed model, by using a general polynomial discretization method in backward and forward-looking (hybrid discretization). By comparing the continuous-time system to its discrete-time counterpart we prove that fixed points and local dynamics do not change, as long as the time step is not too high. Moreover, numerical simulations employing Dynamic Time Warping, cross-correlation, and semblance analysis consistently affirm that enhancing the similarity of quantitative dynamics is achieved by reducing the time step.

Keywords Goodwin model with nonlinear Phillips curve · Local and global dynamics · Hybrid discretization method · Dynamic time warping · Cross-correlation · Semblance analysis

Mathematics Subject Classification 37M · 37N · 39A · 91-10

JEL Classification C62 · C63 · E32

✉ E. Michetti
elisabetta.michetti@unimc.it

M. M. Baldi
mauromaria.baldi@unimc.it

M. Guzowska
malgorzata.guzowska@usz.edu.pl

[1] Department of Economics and Law, University of Macerata, Via Crescimbeni 14, 62100 Macerata, Marche, Italy

[2] Institute of Economics and Finance, University of Szczecin, Adama Mickiewicza 64, 71-101 Szczecin, Pomerania, Poland

Published online: 22 October 2024

1 Introduction

The choice between continuous and discrete time while building dynamic models is a discussed question, especially in economic theory. For instance, the majority of macroeconomic models use differential equations or sets of these equations to describe economic growth. Examples include models proposed by Solow (1956), Swan (1956), Haavelmo (1954), Ramsey (1928), and Goodwin (1967). However, since the majority of economic data is available in discrete time, it is often necessary to consider models expressed in discrete time (difference equations), especially when dealing with applications involving real-world data.

When such needs become prominent, models require to be formalized in discrete time. To the scope, the first way is to construct the model from the beginning by assuming the time is not continuous. Certainly, qualitative and quantitative dynamics, in general, will yield results that differ from those demonstrated by the continuous-time version. This raises potential doubts about the model's ability to accurately depict the phenomenon under study.

As a consequence, researchers began exploring methods and approaches that could facilitate the transition from a satisfying model in continuous time (based on a given target), to its discrete-time counterpart while preserving the same dynamic properties. To pursue this second approach, discretization methods must be used.

Such approaches give rise to important questions to be addressed. For instance, will the equilibria remain unchanged? And what about their local stability properties? If the quantitative dynamics differ, is it possible to measure their *similarity*?

In the present paper, we give an answer to such questions starting from a modified version of a very popular continuous-time growth model, i.e., the Goodwin model (Goodwin 1967). The motivation for modifying the original Goodwin model is to make its behaviour more realistic by introducing a non-linear Phillips curve into the model, following the original idea of Phillips (1958). More precisely, the obtained model is not only a modified version of the standard Goodwin model, but it also represents a generalization of the initial formulation because of the introduction of a parameter, namely $\eta > 0$, measuring the weight the nonlinear term has in the Phillips curve. More in detail, the modified Goodwin model represents a family of systems tending to the standard Goodwin model as long as $\eta \to \infty$.

After introducing the modified Goodwin model, in order to move from continuous to discrete time, a non-standard discretization method is used, namely hybrid discretization (see, for instance, Bosi and Ragot (2012)). The obtained discrete-time model is then investigated with the main goal of comparing equilibria, local stability, and numerical properties.

Our main findings indicate that the use of hybrid discretization maintains the equilibria and their local stability unchanged. On the other hand, when quantitative dynamics are investigated one has to discuss how much solutions differ. More in detail we need to investigate the closeness between the trajectories produced by the discrete model and the curves obtained from the system of differential equations. This question requires careful study and evaluation, taking into account the impact of various elements, including how they change in response to modifications in initial conditions, parameters, and *time steps*.

To appreciate the proximity between the continuous and discrete models herewith proposed, we employ various tools. The most relevant one is the Dynamic Time Warping algorithm (DTW), which aims to align a time series with a reference one in a way that minimizes the sum of distances between corresponding points. Other tools used include the mean error, cross-correlation, as well as semblance analysis. Experimental tests confirm that discrete approximation approaches the continuous model by reducing the step size.

The paper is organized as follows. First, we study the role of the added nonlinear component to the standard Phillip curve on the local and global dynamics of the continuous time system (Sect. 2). Then we move from the continuous time setup to the discrete-time one by applying the hybrid discretization method; the qualitative dynamics of the discrete-time model are then studied and compared to those produced by the continuous time initial version (Sect. 3). Even though equilibria and local qualitative dynamics do not change, in Sect. 4 we discuss the *goodness* of the discretization method by making use of numerical simulations and statistical techniques such as the DTW algorithm, the mean error, cross-correlation, and semblance analysis. Our key observation, as illustrated in the computational results section (Sect. 4) and outlined in the conclusions provided in Sect. 5, is that the orbits of the discrete model tend to align with those of the continuous model as the step size approaches zero. This suggests that the discrete-time approximation performs effectively, provided that the step size is not excessively large.

2 The modified Goodwin model

The Goodwin growth model (Goodwin 1967) is a well-known model that combines aspects of the Harrod-Domar growth model (by Roy F. Harrod (1939) and Evsey Domar (1946)) with the Phillips curve (describing the correlation between reduction in unemployment and increased rates of wage) to explain endogenous economic fluctuations in continuous time. Since Goodwin's publication in 1967, the model has been extensively expanded to incorporate new elements, as demonstrated by several researchers such as Desai (1973), Gandolfo (1997), Vercelli (2000), Sordi and Vercelli (2006), Sordi and Vercelli (2012), and Sordi and Vercelli (2014). In addition to the theoretical approaches, Goodwin's model is also used in practice (see, for instance, Araujo et al. (2019), Matsumoto et al. (2018), Araujo and Moreira (2021), and Santos et al. (2011)).

We recall that the standard Goodwin model is described by the following two-dimensional system S in the variables $v \in [0, 1]$, representing the employment rate, and $u \in [0, 1]$, representing the wage share:

$$S : \begin{cases} \frac{dv}{dt} = [\frac{1}{\sigma} - (\alpha + \beta) - \frac{1}{\sigma}u]v \\ \frac{du}{dt} = [-\alpha + (\rho v - \gamma)]u \end{cases} \tag{1}$$

where $\alpha > 0$ and $\beta > 0$ are growth rates respectively of labour productivity and labour supply, $\sigma > 0$ is the capital/output ratio while $\gamma > 0$ and $\rho > 0$ are related to the variation of real wage rate under the assumption of linear approximation.

We also recall that the standard Goodwin model (1) always admits up to two fixed points as stated in the following remark (see Liu and Elaydi (2001) and Grassetti et al. (2020)).

Remark 1 Consider system (1).

- The origin $E_0 = (0, 0)$ is a hyperbolic saddle point,
- as long as $\sigma(\alpha + \beta) \in (0, 1)$ and $\alpha + \gamma < \rho$, an interior fixed point exists $E_S = (v_s, u_s) = \left(\frac{\alpha+\gamma}{\rho}, 1 - \sigma(\alpha + \beta)\right) \in (0, 1) \times (0, 1)$, whose associated eigenvalues are both purely imaginary, representing a center.

Notice that the function $\dot{w}/w = f(v) = \rho v - \gamma$ involved in the second equation of system (1) represents the standard Phillips curve relation proposed in the original Goodwin's model.

In the present work, we aim to consider that the rate of changes of the wage share not only depends on the employment rate, v, but is also additionally influenced by the labor bill, u. To take into account such evidence, we add a new component to the Pillips curve, namely $g(u)$, thus obtaining

$$\dot{w}/w = f(v) + g(u),$$

where $g(u)$ is assumed to be a continuous and decreasing w.r.t. u. Such an assumption is in accordance with the original idea of Phillips (1958).

According to the previous considerations, the function $g(u)$ can be formalized as follows:

$$g(u) = (1 - u)^{\eta}, \quad \eta > 0, \tag{2}$$

thus satisfying

$$\frac{\partial g}{\partial u} = -\eta(1 - u)^{\eta-1} < 0$$

i.e., workers claim higher wages when they experience a disadvantage in the income distribution.

The modified Goodwin model in continuous time is then described by the following system:

$$CG : \begin{cases} \frac{dv}{dt} = v\left(\frac{1}{\sigma} - \alpha - \beta - \frac{1}{\sigma}u\right) \\ \frac{du}{dt} = u((1 - u)^{\eta} - \alpha - \gamma + \rho v) \end{cases}, \tag{3}$$

where constants α, β, γ, σ, η, and ρ are positive, and the state variables $v \in [0, 1]$ and $u \in [0, 1]$ are respectively the employment rate and the wage share.

Notice that, since $\lim_{\eta\to\infty} g(u) = 0$ then the standard Goodwing model can be seen as a limit form of the modified Goodwin model when the nonlinear component of the Phillips curve tends to zero, i.e., for η approaching infinity. On the other hand, if $\eta \to 0$ then CG tends to CG_0 where the latter is simply obtained by (3) while substituting the second equation with $u(1-\alpha-\gamma+\rho v)$.

2.1 Fixed points and local stability

The fixed points of system CG are summarized in the following proposition.

Proposition 1 *The continuous time dynamical system CG as given by (3) admits up to three fixed points.*

(i) The origin $E_0 = (0, 0)$ is a fixed point for all parameter combinations.
(ii) Assume $\sigma(\alpha+\beta) \in (0,1)$ and $0 < \alpha+\gamma-(\sigma(\alpha+\beta))^\eta < \rho$, then $E^* = (v^*, u^*) = \left(\frac{\alpha+\gamma-(\sigma(\alpha+\beta))^\eta}{\rho}, 1-\sigma(\alpha+\beta)\right)$ is an interior fixed point.
(iii) Assume $\alpha+\gamma < 1$, then one more equilibrium $E_1 = \left(0, 1-(\alpha+\gamma)^{\frac{1}{\eta}}\right)$ is admitted.

Proof The proof is trivially obtained by solving $\frac{dv}{dt} = 0$ and $\frac{du}{dt} = 0$ and by stating conditions such that the equilibria are feasible. □

It is immediate to observe that, differently from the standard Goodwin model in (1), the new formulation may present up to three fixed points.

More precisely the following considerations hold.

The origin is a fixed point for both system S and CG.

Both S and CG exhibit a unique interior equilibrium. Upon comparing the equilibrium values, it is evident that the wage share at equilibrium remains constant, while the associated employment rate decreases, given by $u^* = u_s - \frac{(\sigma(\alpha+\beta))^\eta}{\rho}$, and, as η approaches infinity, $lim_{\eta\to+\infty} u^* = u_s$. Additionally, the associated condition for the feasibility of v is consequently modified. Notice that condition $0 < \alpha+\gamma-(\sigma(\alpha+\beta))^\eta < \rho$ can be restricted to condition $1 < \alpha+\gamma < \rho$ representing parameters combinations such that the interior equilibrium exists for all $\eta > 0$.

System CG may also have an additional fixed point located on the u-axis at which the wage share is zero.

For what it concerns the local stability of the fixed points owned by CG the following proposition holds.

Proposition 2 *Consider system CG as given by (3) and Proposition 1. The local stability of each fixed point, when it exists, follows.*

(i) If $\alpha+\gamma > 1$ and $\sigma(\alpha+\beta) < 1$, then the origin E_0 is a saddle point.
(ii) The interior fixed point E^* is a stable focus.
(iii) If $\alpha+\beta > \frac{(\alpha+\gamma)^{\frac{1}{\eta}}}{\sigma}$ then the equilibrium E_1 is a stable point, while if $\alpha+\beta < \frac{(\alpha+\gamma)^{\frac{1}{\eta}}}{\sigma}$ then E_1 is a saddle point.

Proof To study the local stability of the fixed points of CG we compute the Jacobian matrix and distinguish between the three cases.

(i) For what it concerns the origin, the related Jacobian matrix is given by

$$J(E_0) = \begin{bmatrix} -\alpha - \beta + \frac{1}{\sigma} & 0 \\ 0 & 1 - \alpha - \gamma \end{bmatrix},$$

since $det(J(E_0)) = \frac{(1-\alpha-\gamma)(1-\sigma(\alpha+\beta))}{\sigma}$, if $(1 - \alpha - \gamma) < 0$ and $(1 - \sigma(\alpha + \beta)) > 0$ it results to be negative. In such a case, E_0 is a hyperbolic saddle point.

(ii) We now consider the interior fixed point. The correspondent Jacobian matrix results as follows:

$$J^*(E^*) = \begin{bmatrix} 0 & -\frac{\alpha+\gamma-(\sigma(\alpha+\beta))^{\eta}}{\rho\sigma} \\ \rho(1 - \sigma(\alpha + \beta)) & -\eta(\sigma(\alpha + \beta))^{-1+\eta}(1 - \sigma(\alpha + \beta)) \end{bmatrix},$$

so that the associated characteristic equation is given by:

$$det(\lambda \mathbf{I} - J^*) = \lambda^2 - tr(J^*)\lambda + det(J^*),$$

where

$$tr(J^*) = -\eta(\sigma(\alpha + \beta))^{-1+\eta}(1 - \sigma(\alpha + \beta))$$

and

$$det(J^*) = \frac{(1 - \sigma(\alpha + \beta))(\alpha + \gamma - (\sigma(\alpha + \beta))^{\eta})}{\sigma}.$$

Observe that a pair of complex conjugate eigenvalues emerges only if $\Delta := (tr(J^*))^2 - 4\,det(J^*) < 0$. In this case:

$$\lambda_{1,2} = \frac{tr(J^*)}{2} \pm i\frac{\sqrt{-\Delta}}{2}$$

If $\eta \to 0$ the eigenvalues tend to be purely imaginary and given by

$$\lambda_{1,2} = \pm i\sqrt{\frac{4(1 - \alpha - \gamma)(1 - \sigma(\alpha + \beta))}{\sigma}},$$

the fixed point is not hyperbolic, and no conclusions can be drawn from the linear analysis. If $\eta > 0$, since the Jacobian matrix has a negative Trace and a positive Determinant then the point E^* is locally stable (about the conditions for the local stability related to the trace and the determinant of the Jacobian matrix (Medio and Lines 2001).

(iii) Finally consider the fixed point $E_1 = (0, 1 - (\alpha + \gamma)^{\frac{1}{\eta}})$. The associated Jacobian matrix is as follows:

$$J(E_1) = \begin{bmatrix} -\alpha - \beta + \frac{(\alpha+\gamma)^{\frac{1}{\eta}}}{\sigma} & 0 \\ \rho - (\alpha + \gamma)^{\frac{1}{\eta}}\rho & -\left((\alpha + \gamma)^{\frac{1}{\eta}}\right)^{-1+\eta}\left(1 - (\alpha + \gamma)^{\frac{1}{\eta}}\right)\eta \end{bmatrix}.$$

Eigenvalues of $J(E_1)$ are then given by:

$$\lambda_1 = -\left((\alpha + \gamma)^{\frac{1}{\eta}}\right)^{-1+\eta}\left(1 - (\alpha + \gamma)^{\frac{1}{\eta}}\right)\eta$$

and

$$\lambda_2 = -\alpha - \beta + \frac{(\alpha + \gamma)^{\frac{1}{\eta}}}{\sigma}.$$

Since $\alpha + \gamma < 1$ and $\eta > 0$ then $\lambda_1 < 0$ for all combinations of parameters. Differently, the eigenvalue λ_2 can be both negative (if $\alpha + \beta > \frac{(\alpha+\gamma)^{\frac{1}{\eta}}}{\sigma}$) or positive (if $\alpha + \beta < \frac{(\alpha+\gamma)^{\frac{1}{\eta}}}{\sigma}$). Then E_1 can be a saddle point or a locally stable fixed point. □

By comparing the qualitative dynamics of the Standard Goodwin model to those exhibited by its modified version, it is of interest to observe that the interior equilibrium point becomes stable. From an economic perspective, this ensures long-term convergence, although fluctuations may still emerge.

3 From continuous to discrete time. The hybrid discretization method

After showing the qualitative properties of the continuous-time model, we now apply the hybrid discretization method to system CG as given by (3) in order to provide a discrete version of the modified Goodwin model that preserves the behavior of the original one, i.e., fixed points and local stability.

To the scope, we use the hybrid discretization method as proposed by Bosi and Ragot (2012) that has also been successfully used in Guzowska and Michetti (2018) and Zhang et al. (2010). The resulting two-dimensional discrete-time dynamical system is as follows:

$$DG : \begin{cases} v_{t+1} = \frac{v_t\sigma}{-h+hu_{t+1}+\sigma+h\sigma(\alpha+\beta)} \\ u_{t+1} = u_t + hu_t((1-u_t)^{\eta} - \alpha - \gamma + v_t\rho), \end{cases} \tag{4}$$

where h is a small enough positive constant representing the discretization step.

3.1 Fixed points and local stability

In order to evaluate the goodness of the discretization methods herewith applied, we first determine the fixed points of the system DG. By substituting $u_{t+1} = u_t$ and $v_{t+1} = v_t$ the following Proposition trivially holds.

Proposition 3 *The discrete-time dynamical system DG as given by (4) admits up to three fixed points:*

(i) *the origin* $E_0 = (0, 0)$,
(ii) *an interior fixed point* $E^* = (v^*, u^*) = \left(\frac{\alpha+\gamma-(\sigma(\alpha+\beta))^{\eta}}{\rho}, 1 - \sigma(\alpha + \beta)\right)$,
(iii) $E_1 = \left(0, 1 - (\alpha + \gamma)^{\frac{1}{\eta}}\right)$ *belonging to the border.*

Conditions on parameters for the existence of the three fixed points are the same as stated in Proposition 1 for the continuous time model.

Proposition 3 shows that systems CG and DG admit the same equilibrium points for any given parameter combinations providing that the discretization method herewith used preserves the existence and number of equilibria of the growth model. For what concerns their local stability the following Proposition holds.

Proposition 4 *The local stability properties of the fixed points of the system DG given by (4) follows.*

(i) If $\alpha + \gamma > 1$ *and* $\sigma(\alpha + \beta) < 1$, *then there exists* $h_0 > 0$ *such that origin* E_0 *is a saddle point for all* $h < h_0$.
(ii) There exists $h^* > 0$ *such that* E^* *is a locally stable fixed point* $\forall h \in (0, h^*)$.
(iii) There exists $h_1 > 0$ *such that,* $\forall h < h_1$ *two cases may emerge: if* $\alpha + \beta > \frac{(\alpha+\gamma)^{\frac{1}{\eta}}}{\sigma}$ *then the equilibrium* E_1 *is a stable point, while if* $\alpha + \beta < \frac{(\alpha+\gamma)^{\frac{1}{\eta}}}{\sigma}$ *then* E_1 *is a saddle point.*

Proof To prove the stability properties of the fixed points of system DG we proceed as follows.

(i) We start considering the origin. For $E_0 = (0, 0)$ the Jacobian matrix evaluated at the fixed point is given by

$$J(E_0) = \begin{bmatrix} \frac{\sigma}{\sigma - h(1-\sigma(\alpha+\beta))} & 0 \\ 0 & 1 + h(1 - \alpha - \gamma) \end{bmatrix}$$

and its eigenvalues are $\lambda_1 = \frac{\sigma}{\sigma - h(1-\sigma(\alpha+\beta))}$ and $\lambda_2 = 1 + h(1 - \alpha - \gamma)$. Define $h_0 = -\frac{2}{1-\alpha-\gamma}$, then being $\alpha + \gamma > 1$ and $\sigma(\alpha + \beta) < 1$ simple computations show that $-1 < \lambda_2 < 1 < \lambda_1$ so that E_0 is a saddle point.

(ii) We now consider the fixed point E^*. The associated Jacobian matrix takes the form:

$$J(E^*) = \begin{bmatrix} j_{11} & j_{12} \\ j_{21} & j_{22} \end{bmatrix}, \tag{5}$$

where

$$j_{11} = -\frac{\sigma + h^2(1-\sigma(\alpha+\beta))\left(\alpha+\gamma-(\sigma(\alpha+\beta))^{\eta}\right)}{\sigma},$$
$$j_{12} = -\frac{\left(\alpha+\gamma-(\sigma(\alpha+\beta))^{\eta}\right)\left(h-h^2\eta(\sigma(\alpha+\beta))^{-1+\eta}(1-\sigma(\alpha+\beta))\right)}{\rho\sigma},$$
$$j_{21} = h\rho(1-\sigma(\alpha+\beta)),$$

and

$$j_{22} = 1 - h\eta(\sigma(\alpha+\beta))^{-1+\eta}(1-\sigma(\alpha+\beta)).$$

Hence the corresponding characteristic equation is given by

$$det(\lambda\mathbf{I} - J^*) = \lambda^2 - tr(J^*)\lambda + det(J^*),$$

where

$$tr(J^*) = 2 - \frac{h^2(1-\sigma(\alpha+\beta))\left(\alpha+\gamma-(\sigma(\alpha+\beta))^{\eta}\right)}{\sigma} + \\ -h\eta(\sigma(\alpha+\beta))^{-1+\eta}(1-\sigma(\alpha+\beta)),$$

and

$$det(J^*) = 1 - h\eta(\sigma(\alpha+\beta))^{-1+\eta}(1-\ \sigma(\alpha+\beta)).$$

Consider the local stability conditions in terms of trace and determinant (see. e.g. Medio and Lines (2001)).

If $\eta \to 0$ then $det(J^*) \to 1$ and the fixed point is not hyperbolic.

If $\eta > 0$ then simple computations show that $(1 - tr(J^*) + det(J^*))$ and $(1 - det(J^*))$ are both positive.

Concerning the third condition to be fulfilled for the local stability, we have to verify that

$$\Psi(h) = (1 + tr(J^*) + det(J^*)) > 0.$$

Simple computations show that

$$\Psi(h) = -\frac{(1-\sigma(\alpha+\beta))\left(\alpha+\gamma-(\sigma(\alpha+\beta))^{\eta}\right)}{\sigma}h^2 \\ -2\eta(\sigma(\alpha+\beta))^{-1+\eta}(1-\ \sigma(\alpha+\beta))h + 4 = \\ = -p_1h^2 - p_2h + 4,$$

where

$$p_1 = \frac{(1-\sigma(\alpha+\beta))\left(\alpha+\gamma-(\sigma(\alpha+\beta))^{\eta}\right)}{\sigma}$$

and

$$p_2 = 2\eta(\sigma(\alpha+\beta))^{-1+\eta}(1-\sigma(\alpha+\beta)).$$

Function $\Psi(h)$ is a concave parabola passing through the point $(0,4)$ and with its vertex at $h_v < 0$. Then there exists a $h^* > 0$ such that $\Psi(h) > 0$ for all $h \in (0, h^*)$.

The value of h^* can be easily computed as

$$h^* = \frac{-p_2 + \sqrt{p_2^2 + 16p_1}}{2p_1}.$$

(iii) Finally, for point E_1 we have

$$J(E_1) = \begin{bmatrix} j_{11} & j_{12} \\ j_{21} & j_{22} \end{bmatrix}.$$

where:

$$\begin{aligned} j_{11} &= \frac{\sigma}{\sigma + h\left(-(\alpha+\gamma)^{\frac{1}{\eta}} + \sigma(\alpha+\beta)\right)}, \\ j_{12} &= 0, \\ j_{21} &= -h\left(-1 + (\alpha+\gamma)^{\frac{1}{\eta}}\right)\rho \end{aligned}$$

and

$$j_{22} = 1 - h\left((\alpha+\gamma)^{\frac{1}{\eta}}\right)^{-1+\eta}\left(1-(\alpha+\gamma)^{\frac{1}{\eta}}\right)\eta.$$

The associated eigenvalues are then given by

$$\lambda_1 = \frac{\sigma}{\sigma + h\left(-(\alpha+\gamma)^{\frac{1}{\eta}} + \sigma(\alpha+\beta)\right)}$$

and

$$\lambda_2 = 1 - h\left((\alpha+\gamma)^{\frac{1}{\eta}}\right)^{-1+\eta}\left(1-(\alpha+\gamma)^{\frac{1}{\eta}}\right)\eta.$$

Since $\alpha + \gamma < 1$, then there exists a

$$h_{11} = \frac{1}{\left((\alpha+\gamma)^{\frac{1}{\eta}}\right)^{-1+\eta}\left(1-(\alpha+\gamma)^{\frac{1}{\eta}}\right)\eta} > 0$$

such that $0 < \lambda_2 < 1$ for all $h < h_{11}$.

In relation to the first eigenvalue, we aim to establish conditions under which $|\lambda_1| > 1$, leveraging the inequality $\sigma(\alpha+\beta) < (\alpha+\gamma)^{1/\eta}$. Let $D = \sigma + h\left(-(\alpha+\gamma)^{\frac{1}{\eta}} + \sigma(\alpha+\beta)\right)$, then we can express λ_1 as $\frac{\sigma}{D}$. It is easy to see that if

$$h < \frac{\sigma}{(\alpha+\gamma)^{\frac{1}{\eta}} - \sigma(\alpha+\beta)},$$

then $D > 0$ and so, taking into account that $\sigma(\alpha+\beta) < (\alpha+\gamma)^{1/\eta}$ the denominator is also less than σ. Consequently, $\lambda_1 > 1$. Vice versa, if

$$h > \frac{\sigma}{(\alpha+\gamma)^{\frac{1}{\eta}} - \sigma(\alpha+\beta)},$$

then $D < 0$. In this case, the inequality $|\lambda_1| > 1$ becomes $\frac{\sigma}{D} < -1$ that is satisfied for

$$h < \frac{2\sigma}{(\alpha+\gamma)^{\frac{1}{\eta}} - \sigma(\alpha+\beta)}.$$

Consequently, considering both possibilities, there exists

$$h_{12} = \frac{2\sigma}{\left((\alpha+\gamma)^{\frac{1}{\eta}} - \sigma(\alpha+\beta)\right)}$$

such that $|\lambda_1| > 1$, $\forall h < h_{12}$ and E_1 is a saddle point; otherwise if $\sigma(\alpha+\beta) > (\alpha+\gamma)^{1/\eta}$ then $0 < \lambda_1 < 1$ and E_1 is locally stable. Let $h_1 = \min\{h_{11}, h_{12}\}$ then the statement holds true. □

By using analytical tools our results show that the equilibria and their local stability properties do not change when moving from the continuous-time to the discrete-time model using the hybrid discretization method as long as the time step is not too high. Anyway, quantitative dynamics must be considered to detect the goodness of the discretization method herewith proposed. For this purpose, in the next section, we employ numerical tools with the primary objective of assessing the extent to which the evolution of two systems may differ and examining the impact of the choice of initial conditions and parameter values.

4 Quantitative comparisons

As it has been proved, the fixed points and, in particular, the economically meaningful interior equilibrium point, maintain their local stability properties when moving from a continuous to a discrete-time setup using the hybrid discretization method if the time step involved in the discrete-time model is not too high.

Anyway, although the local qualitative behavior of the two systems is the same, we want to give an answer to the following open questions: if also the quantitative dynamics are the same or if and in which measure they differ.

To assess the approximation of the discretized model to the continuous one, we compare the dynamics of the two models under various parameter settings referred to as scenarios, and focusing on the solutions converging to the interior equilibrium.

A distinguishing feature of this study, in contrast to previous works (e.g., Grassetti et al. (2020)), is the utilization of the Dynamic Time Warping algorithm for comparing the orbits.

The rest of this section is organized as follows: first, we briefly recall the metrics used to compare the discretized model with the continuous one. Then, we introduce the scenarios considered during the computational tests. After that, we summarize the results obtained, both in graphical and tabular form.

In the following, we are going to compare the orbits of a discrete model with those of a continuous one. Theoretically speaking, an orbit of a discrete dynamical system is a set with an infinite number of elements whose cardinality is $\aleph_0$. Vice versa, an orbit of a continuous dynamical system is a set with an infinite number of elements with the cardinality of the continuum. In practice, it is not feasible to make a comparison through the use of a computer because we have to deal with an infinite number of elements and with different cardinalities. Thus, in the following comparisons, we truncate both the orbits at a reasonable time limit $t_{\max}$. Such a value can be any instant of time after the transient phase. We still have to fix the issue that the orbit of the continuous dynamical system has an infinite number of points in $[0,\ t_{\max}]$. In our comparisons, we sample this orbit in the same instants of time of the discrete dynamical system, i.e., with a time step $h < h^*$. In this way, there are $N = \left[\frac{t_{\max}}{h} + 1\right]$ points in $[0,\ t_{\max}]$ for both the orbits. We denote by $x^d = \{x_0^d,\ x_1^d,\ \ldots,\ x_{N-1}^d\}$ the points of the orbit of the discrete dynamical system and by $x^c = \{x_0^c,\ x_1^c,\ \ldots,\ x_{N-1}^c\}$ the corresponding points of the orbit of the continuous dynamical system. Here, the letter x, depending on the context, can either be u, v, or even $(u,\ v)$.

4.1 The error

The error ϵ is just the norm of the difference of the two sampled sequences, i.e.:

$$\epsilon = \|x^c - x^d\|.$$

4.2 The dynamic time warping algorithm

The Dynamic Time Warping (DTW) is a dynamic-programming algorithm that aims to compare two time series $x = \{x_0,\ x_1,\ \ldots,\ x_{N-1}\}$ and $y = \{y_0,\ y_1,\ \ldots,\ y_{M-1}\}$ not necessarily of the same length (in fact, $M \neq N$ in principle) but with the same time step (Rabiner and Juang 1993; Müller 2007). Using a distance metric (typically the l1 or l2 norm), the DTW algorithm seeks the minimum warping path, which is a path minimizing the distance. For details on the application of this algorithm, see, for instance, Smidtaite et al. (2023). A warping path is a sequence of indexes of the two

time series satisfying boundary, monotonicity, and step-size conditions (Müller 2007). Thus, the output of the DTW algorithm is a score equal to the sum of the distances of the couples of points involved in the optimal warping path. Consequently, this score provides a measure of the similarity of the two signals. In particular, the lower the score, the closer the two signals.

4.3 Cross correlation

Cross-correlation is a widespread indicator in signal processing that aims to measure the similarity of two time series (examples of applications are in Kristoufek (2016) and Hua and Wu (2023)). Given a particular instant of time $n \in \mathbb{N}$ and two time series x and y, the cross correlation at time n between x and y is defined as:

$$R_{xy}(n) = \sum_{m=-\infty}^{+\infty} x_m y_{n+m}.$$

If more than an instant of time is considered, the result is a vector of cross-correlation coefficients, where each element in the vector is associated to an instant of time.

4.4 Semblance analysis

Semblance analysis describes the correlation between two signals both in terms of time and wavelength. The result is a matrix of values between -1 and 1. One axis of the matrix refers to the time, while the other one to the wavelength. If an element of the matrix is positive, then the two time series at that time and wavelength are correlated. If negative, they are anti-correlated, and if zero, they are uncorrelated. An application of semblance analysis can be found in Jacob and Urban (2016).

4.5 Computational results

We conducted our computational analysis using Matlab. Given the considerable number of parameters describing the model, we decided to test the model under different combinations of parameters. We name scenario each combination of parameters. In Table 1, we show the parameter values of each scenario.

In Table 2, we show the results for each scenario, starting from $(v_0, u_0) = (1/4, 1/4)$. As previously mentioned, the number of points in the time interval $[0, t_{\max}]$ depends on h and is given by $N = \left[\frac{t_{\max}}{h} + 1\right]$. In Table 2, we are comparing different time series with different numbers of points. Thus, to make this comparison fair, we need to scale the results obtained from computations by the number of points N in order to get a mean score. In particular, the error in column 3 is given by ϵ/N. The DTW in columns 4 and 5 is given by the score of the DTW algorithm (computed both using the l_1 and l_2 norm) divided by N. Finally, columns 6 and 7 show the mean cross correlation respectively for v and u. This is given by the sum of the elements in the array of the cross-correlation divided by N.

Table 1 Parameter values for the considered scenarios

Scenario	α	β	γ	η	ρ	σ
1	0.8	0.1	0.4	2	2	0.5
2	0.7	0.4	0.5	2.5	3	0.5
3	0.4	0.4	1	3	3	1
4	0.3	0.3	0.5	2	2	1
5	0.4	0.4	1.5	3	2	1
6	0.1	0.8	0.6	1	1.5	0.7
7	0.6	0.3	0.7	4	2	0.8
8	0.5	0.5	0.5	0.5	0.5	0.7
9	0.5	0.5	0.5	0.5	1	0.8
10	0.5	0.5	0.5	2.5	1	0.8

Table 2 Indicators' results

Scenario	h	Error	DTW l_2	DTW l_1	Xcorr v	Xcorr u
1	1.0	6.88×10^{-3}	1.99×10^{-2}	2.46×10^{-2}	1.03×10^{1}	1.21×10^{1}
	0.8	3.83×10^{-3}	1.16×10^{-2}	1.47×10^{-2}	1.27×10^{1}	1.51×10^{1}
	0.4	9.77×10^{-4}	4.09×10^{-3}	5.14×10^{-3}	2.52×10^{1}	2.99×10^{1}
	0.1	1.02×10^{-4}	1.12×10^{-3}	1.41×10^{-3}	1.00×10^{2}	1.19×10^{2}
2	1.0	1.45×10^{-3}	4.21×10^{-3}	5.56×10^{-3}	4.34×10^{0}	8.15×10^{0}
	0.8	8.77×10^{-4}	2.85×10^{-3}	3.74×10^{-3}	5.41×10^{0}	1.02×10^{1}
	0.4	2.39×10^{-4}	1.38×10^{-3}	1.80×10^{-3}	1.07×10^{1}	2.02×10^{1}
	0.1	2.69×10^{-5}	5.24×10^{-4}	6.67×10^{-4}	4.28×10^{1}	8.05×10^{1}
3	1.0	4.90×10^{-4}	1.18×10^{-3}	1.57×10^{-3}	3.52×10^{0}	1.60×10^{0}
	0.8	3.49×10^{-4}	8.96×10^{-4}	1.20×10^{-3}	4.38×10^{0}	1.99×10^{0}
	0.4	1.22×10^{-4}	4.13×10^{-4}	5.52×10^{-4}	8.69×10^{0}	3.95×10^{0}
	0.1	1.44×10^{-5}	9.55×10^{-5}	1.26×10^{-4}	3.46×10^{1}	1.57×10^{1}
4	1.0	5.81×10^{-4}	1.72×10^{-3}	2.21×10^{-3}	2.03×10^{0}	6.53×10^{0}
	0.8	4.19×10^{-4}	1.41×10^{-3}	1.81×10^{-3}	2.53×10^{0}	8.14×10^{0}
	0.4	1.52×10^{-4}	7.33×10^{-4}	9.38×10^{-4}	5.04×10^{0}	1.62×10^{1}
	0.1	2.03×10^{-5}	1.99×10^{-4}	2.55×10^{-4}	2.00×10^{1}	6.45×10^{1}
5	1.0	1.59×10^{-2}	4.46×10^{-2}	5.45×10^{-2}	1.96×10^{1}	1.47×10^{0}
	0.8	6.09×10^{-3}	1.13×10^{-2}	1.42×10^{-2}	2.36×10^{1}	1.81×10^{0}
	0.4	1.76×10^{-3}	3.86×10^{-3}	4.77×10^{-3}	4.63×10^{1}	3.55×10^{0}

The results in Table 2 clearly show how the approximation given by the discrete model improves when h is reduced. In fact, the mean error in column 3 decreases when h is decreased. A similar trend can be observed in the columns reporting DTW results, thus confirming the improvement of the discrete-time series when h decreases. The columns associated to the cross-correlation analysis tell us that the mean correlation between the discrete and continuous orbits increases when h decreases.

Table 2 continued

Scenario	h	Error	DTW l_2	DTW l_1	Xcorr v	Xcorr u
	0.1	2.06×10^{-4}	9.47×10^{-4}	1.16×10^{-3}	1.83×10^{2}	1.41×10^{1}
6	1.0	6.44×10^{-4}	2.42×10^{-3}	3.04×10^{-3}	1.50×10^{-1}	6.01×10^{0}
	0.8	4.70×10^{-4}	1.96×10^{-3}	2.44×10^{-3}	1.86×10^{-1}	7.49×10^{0}
	0.4	1.75×10^{-4}	1.03×10^{-3}	1.27×10^{-3}	3.64×10^{-1}	1.49×10^{1}
	0.1	2.55×10^{-5}	2.85×10^{-4}	3.60×10^{-4}	1.44×10^{0}	5.93×10^{1}
7	1.0	2.74×10^{-3}	4.52×10^{-3}	5.97×10^{-3}	1.06×10^{1}	3.04×10^{0}
	0.8	1.81×10^{-3}	2.93×10^{-3}	3.88×10^{-3}	1.32×10^{1}	3.78×10^{0}
	0.4	5.84×10^{-4}	1.22×10^{-3}	1.62×10^{-3}	2.61×10^{1}	7.50×10^{0}
	0.1	6.90×10^{-5}	3.37×10^{-4}	4.36×10^{-4}	1.04×10^{2}	2.98×10^{1}
8	1.0	2.50×10^{-4}	1.07×10^{-3}	1.39×10^{-3}	4.38×10^{0}	3.60×10^{0}
	0.8	1.74×10^{-4}	8.32×10^{-4}	1.07×10^{-3}	5.46×10^{0}	4.49×10^{0}
	0.4	5.63×10^{-5}	3.96×10^{-4}	4.95×10^{-4}	1.09×10^{1}	8.92×10^{0}
	0.1	6.44×10^{-6}	1.15×10^{-4}	1.44×10^{-4}	4.32×10^{1}	3.55×10^{1}
9	1.0	2.94×10^{-4}	1.64×10^{-3}	2.11×10^{-3}	4.82×10^{-1}	1.78×10^{0}
	0.8	2.07×10^{-4}	1.29×10^{-3}	1.66×10^{-3}	5.98×10^{-1}	2.22×10^{0}
	0.4	7.17×10^{-5}	6.20×10^{-4}	8.07×10^{-4}	1.18×10^{0}	4.39×10^{0}
	0.1	9.21×10^{-6}	1.57×10^{-4}	2.11×10^{-4}	4.66×10^{0}	1.74×10^{1}
10	1.0	1.41×10^{-3}	2.07×10^{-3}	2.69×10^{-3}	7.03×10^{0}	1.55×10^{0}
	0.8	9.95×10^{-4}	1.74×10^{-3}	2.26×10^{-3}	8.75×10^{0}	1.93×10^{0}
	0.4	3.45×10^{-4}	8.75×10^{-4}	1.14×10^{-3}	1.73×10^{1}	3.83×10^{0}
	0.1	4.22×10^{-5}	2.19×10^{-4}	2.80×10^{-4}	6.89×10^{1}	1.52×10^{1}

Inspired by these results, we decided to perform a more detailed analysis. We concentrated on scenario 5 because it is the scenario with the highest values of the DTW algorithm. In Fig. 1, we plot the orbit of v and u for the continuous and discrete models, starting from $(v_0,\ u_0) = (1/4,\ 1/4)$, and with different values of h. It is clear from these pictures that the discrete orbit is significantly different from the continuous one for the highest values of h. This difference is dramatically reduced when $h = 0.1$.

A similar trend can also be appreciated from a two-dimensional analysis of the orbit. To this purpose, in Fig. 2 we compare the phase portrait of two orbits, starting from $(v_0,\ u_0) = (0.4,\ 0.4)$ and $(v_0,\ u_0) = (0.6,\ 0.6)$.

It is evident from Fig. 2 that the discrete model yields a coarse approximation for a high value of h, but this approximation significantly improves if h is reduced. Figure 2 also confirms that all the orbits converge to the interior fixed point, even when the quality of the approximation is not accurate.

Another interesting comparison is provided in Fig. 3. Here, we have reported the mean error and the mean DTW score (computed using both the l-1 and l-2 norm) for scenario 5, again starting from $(u_0,\ v_0) = (1/4,\ 1/4)$ and varying h between 0.1 and 1.

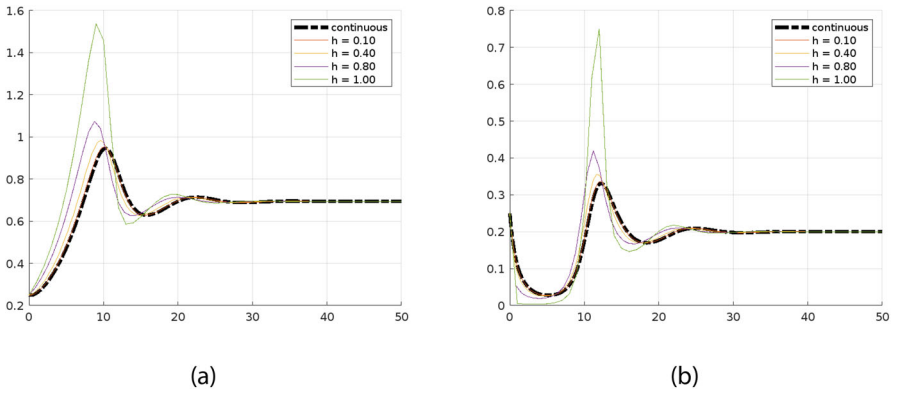

Fig. 1 Continuous and discrete orbits for scenario 5 concerning v (panel a) and u (panel b)

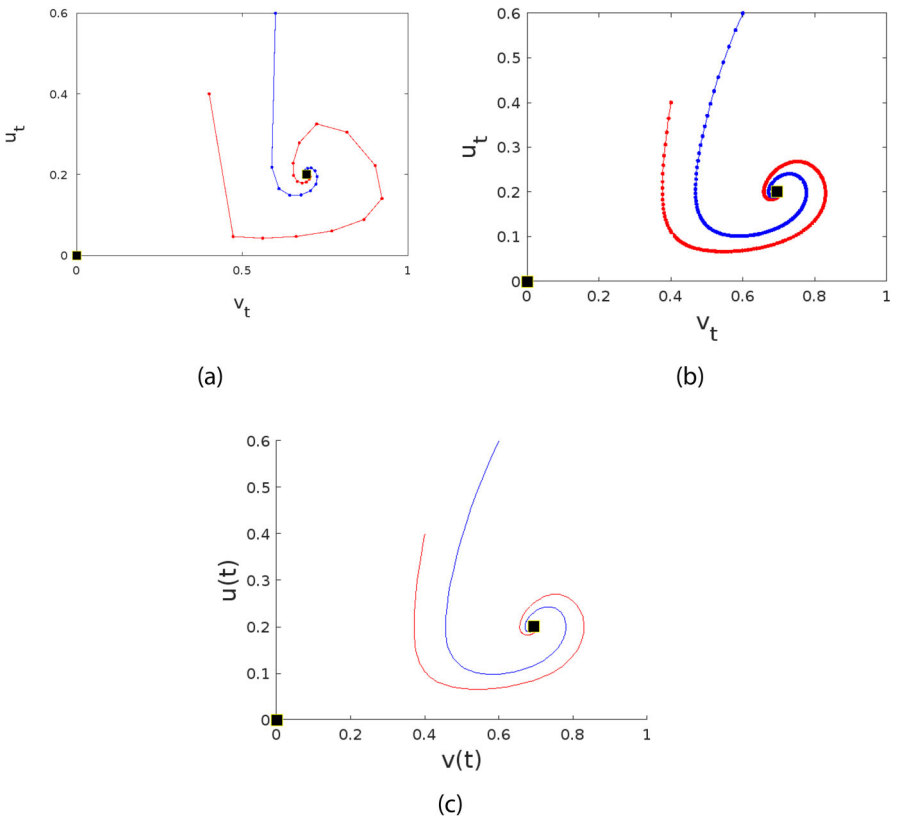

Fig. 2 A comparison of phase portraits for scenario 5 between the discrete model with $h = 1$ (panel a), $h = 0.1$ (panel b), and the continuous model (panel c)

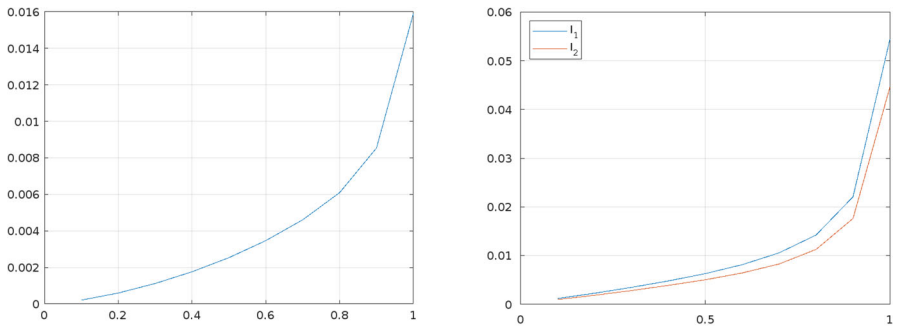

Fig. 3 The mean error (panel a) and the mean DTW score (panel b) for scenario 5, with h varying between 0.1 and 1

Again, the conclusion confirms the previous evidence: both the error and the DTW scores dramatically reduce when h is decreased.

Regarding the DTW algorithm, it is worthwhile to present a graphical representation of the results. In this regard, Fig. 4 shows the assignments of points resulting from the DTW algorithm for scenario 5 between the continuous and discrete orbits. For example, the upper plot in Fig. 4a overlaps the orbits of v_t (in yellow) with $h = 1$ and $v(t)$ (in blue), both starting from $v_0 = 1/4$ (and $u_0 = 1/4$).

As illustrated in the lower plot in Fig. 4a, the DTW algorithm stretches the v_t orbit in a way that it assumes a shape as similar as possible to $v(t)$. As a consequence, the peaks of the two orbits become aligned. The same procedure applies in Fig. 4b, but this time v_t is computed with a step size of 0.1. As already witnessed by the previous figures, with this choice of h the discrete orbit tends to the continuous one. Consequently, the DTW algorithm does not perform an appreciable stretching, thus yielding a lower score. Similar considerations hold for Fig. 4c, d.

Finally, in Fig. 5, we show graphical results from semblance analysis for $h = 1$ and $h = 0.1$. Semblance analysis shows the correlation between two datasets as a function of both time and wavelength. In Figure 5, anticorrelation (s=-1) is displayed in blue, zero correlation (s=0) in green, and positive correlation (s=+1) in red colour. In both cases ($h = 1$ and $h = 0.1$), the image shows the correlation between the continuous model and the discrete one, which is mostly red (implying a strong positive correlation).

5 Conclusion

Introducing a nonlinear term to the Phillips curve has led to a new formulation of the Goodwin growth model. In contrast to the standard model, the modified Goodwin model can exhibit up to three equilibria, including an additional fixed point on the boundary. Naturally, the inclusion of the nonlinear term in the Phillips curve alters the parameter conditions for the existence of these fixed points.

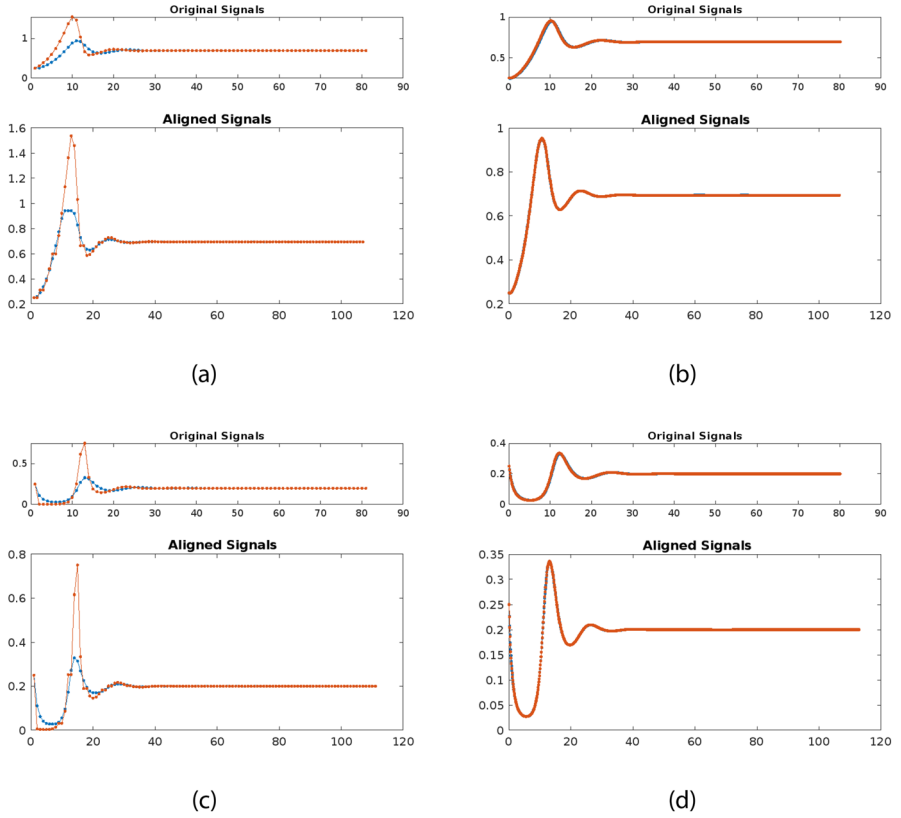

Fig. 4 The final assignments of the DTW algorithm for scenario 5 involving v_t with $h = 1$ (panel a), v_t with $h = 0.1$ (panel b), u_t with $h = 1$ (panel c), and u_t with $h = 0.1$ (panel d)

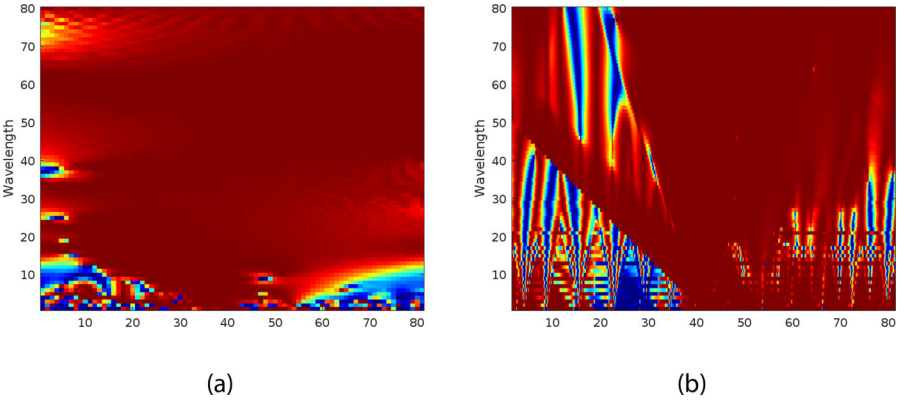

Fig. 5 Semblance analysis results for scenario 5 with $h = 1$ (panel a) and $h = 0.1$ (panel b)

In any case, considering the economically significant equilibrium, namely the interior fixed point, we observe that even if the wage share remains constant, the equilibrium employment rate decreases due to disadvantages in income distribution. Moreover, a surprising effect on the local stability properties of the economically meaningful fixed point emerges; it ceases to be a center and instead becomes a stable focus. This alteration in local stability is noteworthy from an economic perspective as it endows the economy with endogenous forces ensuring the convergence of economic variables in the long run. Furthermore, endogenous fluctuations become apparent, aligning with typical patterns observed in economic data. These findings hold true for both continuous-time and discrete-time frameworks, provided the time step is sufficiently small.

In our comparisons of quantitative dynamics, we presented various scenarios and assessed the effectiveness of the employed discretization method concerning the economically meaningful equilibrium through numerical simulations. Utilizing different computational techniques, primarily Dynamic Time Warping in conjunction with other metrics, we demonstrate that the discrete-time model continues to be a reliable approximation of the continuous-time model, even from a quantitative perspective, provided that the time step is not excessively high.

Acknowledgements Malgorzata Guzowska has been financed within the framework of the program of the Minister of Science and Higher Education under the name "Regional Excellence Initiative" in the years 2019–2022, project number 001/RID/2018/19, the amount of financing PLN 10,684,000.00. Mauro Maria Baldi and Elisabetta Michetti have been financed by the European Union - NextGenerationEU under the Italian Ministry of University and Research (MUR) National Innovation Ecosystem grant ECS00000041 - VITALITY - CUP D83C22000710005.

References

Araujo, R., Dávila-Fernández, M., Moreira, H.: Some new insights on the empirics of Goodwin's growth-cycle model. Struct. Chang. Econ. Dyn. **51**, 42–54 (2019)

Araujo, R., Moreira, H.: Testing a Goodwin's model with capacity utilization to the US economy. Nonlinearities in Econ. Interdiscip. Approach Econ. Dyn. Growth Cycles (2021). https://doi.org/10.1007/978-3-030-70982-2_19

Bosi, S., Ragot, L.: Time representation in economics. Theor. Econ. Lett. **2**(1), 10–15 (2012)

Desai, M.: Growth cycles and inflation in a model of the class struggle. J. Econ. Theory **6**(6), 527–545 (1973)

Domar, E.: Capital expansion, rate of growth, and employment. Econ. J. Econ. Soc. (1946). https://doi.org/10.2307/1905364

Gandolfo, G.: Economic Dynamics: Study Edition. Springer, ??? (1997)

Grassetti, F., Guzowska, M., Michetti, E.: A dynamically consistent discretization method for Goodwin model. Chaos, Solitons & Fractals **130**, 109420 (2020)

Guzowska, M., Michetti, E.: Local and global dynamics of ramsey model: from continuous to discrete time. Chaos: Interdiscip. J. Nonlin. Sci. **10**(1063/1), 5024337 (2018)
Goodwin, R.: A Growth Cycle: Socialism, Capitalism and Economic Growth, 1967, ED. CH Feinstein. In: Essays in Economic Dynamics, pp. 165–170. Springer, ??? (1967)
Haavelmo, T.: A study in the theory of economic evolution. J. Inst. Theor. Econ. 361–363 (1954)
Harrod, R.: An essay in dynamic theory. Econ. J. **49**(193), 14–33 (1939)
Hua, M., Wu, Y.: Cross-correlated sine-wiener noises-induced transitions in a tumor growth system. Commun. Nonlinear Sci. Numer. Simul. **126**, 107489 (2023)
Jacob, R., Urban, T.: Ground-penetrating radar velocity determination and precision estimates using common-midpoint (cmp) collection with hand-picking, semblance analysis and cross-correlation analysis: A case study and tutorial for archaeologists. Archaeometry **58**(6), 987–1002 (2016)
Kristoufek, L.: Power-law cross-correlations estimation under heavy tails. Commun. Nonlinear Sci. Numer. Simul. **40**, 163–172 (2016)
Liu, P., Elaydi, S.: Discrete competitive and cooperative models of lotka-volterra type. J. Comput. Anal. Appl. **3**, 53–73 (2001)
Medio, A., Lines, M.: Nonlinear dynamics: a primer. Cambridge University Press, ??? (2001)
Matsumoto, A., Merlone, U., Szidarovszky, F.: Goodwin accelerator model revisited with fixed time delays. Commun. Nonlinear Sci. Numer. Simul. **58**, 233–248 (2018)
Müller, M.: Information Retrieval for Music and Motion. Springer, ??? (2007)
Phillips, A.: The relation between unemployment and the rate of change of money wage rates in the united kingdom, 1861–1957. Economica **25**(100), 283–299 (1958)
Ramsey, F.: A mathematical theory of saving. Econ. J. **38**(152), 543–559 (1928)
Rabiner, L., Juang, B.: Fundamentals of speech recognition. Prentice-Hall Signal Processing Series: Advanced monographs. PTR Prentice Hall, ??? (1993)
Solow, R.: A contribution to the theory of economic growth. Q. J. Econ. **70**(1), 65–94 (1956)
Santos, A.P., Silva, R., Alcaniz, J.S., Anselmo, D.H.A.L.: Kaniadakis statistics and the quantum h-theorem. Phys. Lett. A **375**(3), 352–355 (2011)
Smidtaite, R., Saunoriene, L., Ragulskis, M.: Detection of lag synchronization based on matrices of delayed differences. Commun. Nonlinear Sci. Numer. Simul. **116**, 106864 (2023)
Sordi, S., Vercelli, A.: Financial fragility and economic fluctuations. J. Econ. Behav. Organ. **61**(4), 543–561 (2006)
Sordi, S., Vercelli, A.: Heterogeneous expectations and strong uncertainty in a minskyian model of financial fluctuations. J. Econ. Behav. Organ. **83**(3), 544–557 (2012)
Sordi, S., Vercelli, A.: Unemployment, income distribution and debt-financed investment in a growth cycle model. J. Econ. Dyn. Control **48**, 325–348 (2014)
Swan, T.: Economic growth and capital accumulation. Econ. Record **32**(2), 334–361 (1956)
Vercelli, A.: Structural financial instability and cyclical fluctuations. Struct. Chang. Econ. Dyn. **11**(1–2), 139–156 (2000)
Zhang, Z., Kostyukova, O., Zhang, Y., Chong, K.: Hybrid discretization method for time-delay nonlinear systems. J. Mech. Sci. Technol. **24**, 731–741 (2010)